

Slow Magnetic Relaxation in a Lanthanide-[1]Metallocenophane Complex

Trevor P. Latendresse, Nattamai S. Bhuvanesh, and Michael Nippe*¹

Department of Chemistry, Texas A&M University, 3255 TAMU, College Station, Texas 77843, United States

S Supporting Information

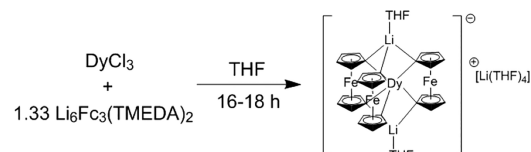
ABSTRACT: The first example of a lanthanide metallocenophane complex has been isolated as $[\text{Li}(\text{THF})_4]\text{[DyFc}_3\text{Li}_2(\text{THF})_2]$ (**1**). The molecular structure of complex **1** differs dramatically from those of main group and transition metal ferrocenophane complexes and features a distorted trigonal prismatic geometry around the Dy(III) ion and close intramolecular Dy...Fe distances. Furthermore, complex **1** exhibits all characteristics of a soft single-molecule magnet.

Metallocenophanes, or ansa-metallocenes, are an intriguing class of compounds that attract significant attention, especially with respect to organometallic catalysis. Within the class of metallocenophane compounds,¹ ferrocenophanes are being most intensively investigated. The isolation and structural characterization of ferrocenophanes is a challenging yet intriguing task for synthetic chemists. The highly strained molecular structures of especially [1]ferrocenophanes² typically result in characteristic reactivity patterns that are driven thermodynamically by release of the ring strain associated with small ansa-bridges.³ Consequently, [1]ferrocenophane complexes have found ample use in homogeneous catalysis and in ring-opening polymerization (ROP) chemistry, where they have been employed as the monomeric unit in route to high molecular weight metallopolymers.⁴

To date, several examples of [1]ferrocenophanes have been reported that feature bonds to either main group elements or transition metal ions. Structurally characterized examples include compounds with bridging atoms from group 13 (B, Al),^{2b,5} group 14 (Si, Ge, Sn),^{6,2d,7} group 15 (P, As),^{2d,8} group 16 (S, Se),^{2c,9} as well as diamagnetic (Zr, Ni, Pd, Pt)¹⁰ and paramagnetic (Fe, Mn)¹¹ transition metal complexes (see Figure 1 for selected examples). Importantly, [1]-

ferrocenophanes possessing f-block elements in the bridgehead have remained largely unexplored. Ephritikhine et al. reported the only known actinide [1]ferrocenophane complex, $[\text{Li}_2\text{UFc}_3(\text{py})_3]\cdot\text{py}$, in which the paramagnetic U(IV) ion is surrounded by three diamagnetic ferrocenophane moieties in a distorted C_3 geometry.¹² The molecular structure of $[\text{Li}_2\text{UFc}_3(\text{py})_3]\cdot\text{py}$ is distinct from those of traditional main group [1]ferrocenophanes in that the typical distortion of the carbocyclic rings is not observed. The distortion, and thus the degree of ring strain, is quantified by the angle formed by the intersection of the planes of the carbocyclic rings (α) as well as the $\text{Cp}^C\text{-Fe-Cp}^C$ (Cp^C = Cp centroid) angle (δ) (see Scheme 1). In detail, $[\text{Li}_2\text{UFc}_3(\text{py})_3]$ features δ values of around 178.5°

Scheme 1. Preparation of 1



indicating a lack of significant ring strain that is most likely due to the less efficient orbital overlap between the U ion and Cp-ring C atoms. Another intriguing structural detail are the close direct through space distances ($d(\text{U}\cdots\text{Fe}) = 3.14(2)$ Å) between the central U(IV) ion and the surrounding low-spin Fe(II) ions that led the authors to hypothesize that heterometallic dative interactions between these centers are possible. The structural variation of $[\text{Li}_2\text{UFc}_3(\text{py})_3]\cdot\text{py}$ from traditional [1]ferrocenophanes opens up new avenues in studies of the reactivity and physical properties of novel f-block-[1]ferrocenophane complexes.

Inspired by these observations, our group became interested in expanding f-block-[1]ferrocenophane chemistry to include lanthanide ions into the bridgehead with a particular focus on the development of new classes of heterometallic lanthanide-transition metal based single-molecule magnets (SMMs). Over the last 2 decades, discrete molecules containing one or more lanthanide ions have received significant interest in the field of molecular magnetism due to the large single ion anisotropy and the unquenched orbital angular momentum of lanthanide ions.¹³ Bistability of the maximum m_j ground states and large energy separations to first and higher excited states has led to lanthanide complexes possessing high effective barriers to

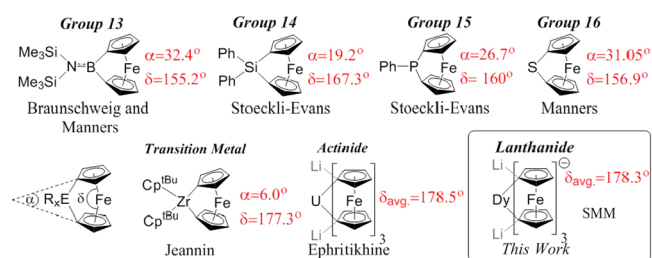


Figure 1. Representative examples of structurally characterized [1]ferrocenophane complexes.

Received: February 14, 2017

Published: June 7, 2017

magnetization reversal (U_{eff}) and consequently significant magnetic hysteresis, lending them to potential use in data storage and processing.

Herein, we report the synthesis, structural, and magnetic characterization of $[\text{Li}(\text{THF})_4][\text{DyFc}_3(\text{THF})_2\text{Li}_2]$ (**1**), which represents the first example of a lanthanide-[1]ferrocenophane complex. The synthesis of **1** is accomplished via the salt elimination reaction between DyCl_3 with 1.3 equiv of $[\text{Fe}(\eta^5\text{-C}_5\text{H}_4)_2]_3\text{Li}_6(\text{TMEDA})_2^{14}$ (TMEDA = tetramethylethylenediamine) in THF at room temperature (Scheme 1). Separation of the salt byproducts via filtration and removal of the THF from the filtrate, affords crude **1** as a red-orange powder that can be further purified by washings of hexanes. Recrystallization from THF/pentane mixtures at -27°C allows for the isolation of compound **1** as pyrophoric orange plate crystals in 20% yields. Notably, **1** can also be prepared using DyI_3 as the lanthanide precursor but the higher solubility of $\text{LiI}(\text{THF})_x$ salts (as compared to LiCl) impedes the isolation of pure **1**.

Compound **1** crystallizes in the monoclinic space group $P2_1/c$ with an exceptionally anisotropic unit cell ($a = 11.3810(9)\text{ \AA}$; $b = 63.671(5)\text{ \AA}$; $c = 13.7280(11)\text{ \AA}$). The molecular structure of **1** (Figure 2, Table S1, S2) shows the central Dy(III) ion

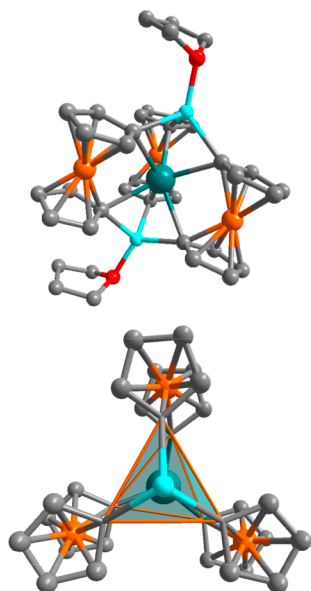


Figure 2. Molecular structure of one monoanionic $[\text{DyFc}_3(\text{THF})_2\text{Li}_2]^-$ molecule in crystals of **1** (top) and view down the Li–Dy–Li axis (bottom, coordinated THF molecules removed). Teal = Dy, orange = Fe, blue = Li, gray = C, red = oxygen. Hydrogen atoms and counteranion have been omitted for clarity.

surrounded by three ferrocenophane moieties each coordinated in the $1'1'$ fashion, promoting a distorted C_3 geometry. Two Li^+ ions reside in the axial positions above and below the equatorial plane inside a tricoordinate “pocket” formed by the C_1 -atoms of the carbocyclic rings and are coordinated by an additional THF ligand. The unit cell of **1** contains two crystallographically unique Dy(III) sites (Dy(1) and Dy(2)), each having subtle differences in the ligand field geometry. Both Dy(1) and Dy(2) have similar average Dy–C distances (Dy– C_{avg} : 2.547[5] \AA for Dy(1)); 2.544[5] \AA (for Dy(2)) ranging between 2.532(5)–2.564(5) \AA and 2.536(5)–2.552(5) \AA , respectively. The average $\text{C}_{\text{Cp}}\text{–Dy–C}_{\text{Cp}}$ angles are 81.02° for Dy(1) and 80.98° for Dy(2), respectively. Coordination of Li^+

is also comparable between the two molecules with average Li–C bond distances of 2.21[1] and 2.22[1] \AA . Most interesting are the intramolecular Dy \cdots Fe distances that are in the range of 3.185(4)–3.262(4) \AA . These values represent some of the shortest Fe \cdots Ln distances reported for heterometallic Fe–lanthanide complexes. Inspection down the approximate local C_3 axis of **1** (Figure 2 bottom), displays the six C_1 donors of the three ferrocenophane ligands are arranged in a distorted trigonal prismatic geometry around the Dy ion. The average twist angle of 12° and 9° for Dy(1) and Dy(2), respectively, suggests significant distortion from ideal trigonal prismatic geometry but is notably less than the twist angle observed for $[\text{Li}_2\text{UFc}_3(\text{py})_3]\cdot\text{py}$ (23°).

The amount of distortion of the carbocyclic rings can be directly correlated to the amount of strain present in [1]ferrocenophane complexes. Similarly to $[\text{Li}_2\text{UFc}_3(\text{py})_3]$, **1** does not display large distortions of the carbocyclic rings with very small α ($<1^\circ$) and linearity approaching averaged δ (178.3°) values, indicating very little ring strain. These values deviate dramatically from those of highly strained main group [1]ferrocenophane complexes, FcSiPh_2 ($\delta = 167.3^\circ$) and $\text{FcBN}(\text{SiMe}_3)_2$ ($\delta = 155.2^\circ$) and are indicative of significantly less efficient orbital overlap between Dy and C_{ring} atoms.

The temperature dependence of the static magnetic properties of **1** were probed by direct current (dc) magnetic susceptibility measurements under an applied field of 1000 Oe in the temperature range from 2 to 300 K (Figure 3). The $\chi_{\text{M}}T$

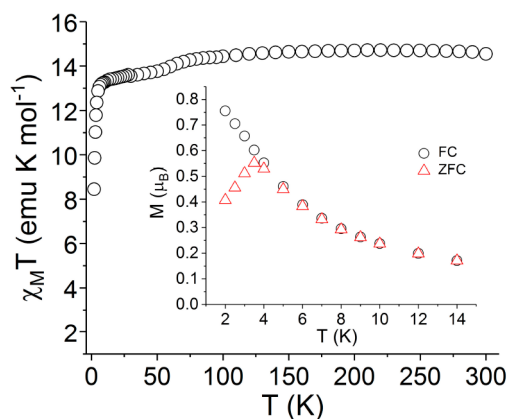


Figure 3. Temperature dependence of $\chi_{\text{M}}T$ for **1** (1000 Oe; 2–300 K). Inset: Temperature dependence of field cooled (black) and zero field cooled (red) magnetization for **1** (1000 Oe).

value at 300 K of 14.54 $\text{emu}\cdot(\text{K}/\text{mol})$ is slightly higher but close to the expected value (14.17 $\text{emu}\cdot(\text{K}/\text{mol})$) for a single noninteracting Dy(III) ion ($^6\text{H}_{15/2}$, $S = 5/2$, $L = 5$, $g = 4/3$). Upon decreasing the temperature, the $\chi_{\text{M}}T$ value remains nearly constant until 65 K, below which a slight decrease is observed. A more rapid decrease is observed around 5 K, reaching a minimum value of 8.45 $\text{emu}\cdot(\text{K}/\text{mol})$ at 2 K. The low temperature decrease in the $\chi_{\text{M}}T$ value is commonly observed for mononuclear lanthanide-based SMMs and can be attributed to depopulation of the stark sublevels and/or weak intermolecular antiferromagnetic coupling. Steep decreases may be indicative of blocking of the magnetization (lowest temperature regime). To probe the occurrence of magnetic blocking in **1**, a zero field cooled (ZFC) magnetization measurement was performed under an 1000 Oe applied dc field (Figure 3 inset). The ZFC and FC curves nearly coincide

until 4 K, below which the ZFC magnetization displays a sharp decrease, reaching a value of $0.4 \mu_B$ at 2 K. The location of the maximum in the ZFC magnetization curve suggests the presence of magnetic blocking in **1** up to temperatures (T_B) of around 3.5 K.^{13g,15} Variable temperature magnetization vs field measurements (Figure S1) indicate that magnetic saturation is approximately reached at 4 T were the magnetization reaches a value of $5.45 \mu_B$ (maximum $5.58 \mu_B$ at 7 T). The value is smaller than the expected $10 \mu_B$, suggesting that the degeneracy of the ${}^6\text{H}_{15/2}$ ground states has been broken by crystal field effects. Furthermore, the magnetically highly anisotropic nature of the Dy(III) ion results in the observed nonsuperposition of the M vs H/T curves (Figure S2).

The dynamic magnetic properties of **1** were probed by variable temperature alternating current (ac) magnetic susceptibility measurements in the absence of an applied dc field between 1 and 1000 Hz. The out-of-phase component of the molar ac susceptibility (χ_M'') (6–20 K Figure 4; see Figure

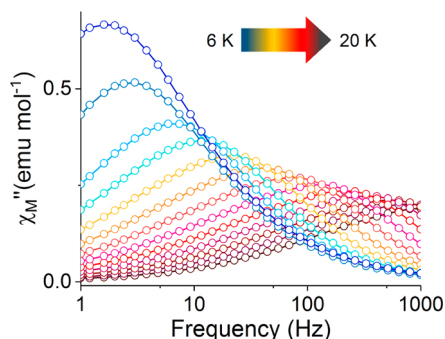


Figure 4. Temperature dependence of the out-of-phase component (χ_M'') of the ac susceptibility of **1** under 0 Oe applied dc field in the temperature range 6–20 K.

S3 for χ_M' and χ_M'' for 1.8–20 K) shows a single peak within the frequency range, indicating that the reversal of the magnetization of **1** is slower than the oscillation of the alternating magnetic field. The frequency of the out-of-phase signal remains temperature independent up to 4 K, upon which the signal begins to shift toward higher frequencies, eventually moving past the experimental 1000 Hz limit at 20 K. The temperature independent nature of χ_M'' below 6 K is indicative of significant contributions from thermally unassisted quantum tunneling processes to the reorientation of the magnetic spin states. To minimize quantum tunneling through intermolecular interactions, magnetically dilute samples of **1** were prepared (compound **3**) (Dy:Y = 1:11.7) (see ESI for details). In fact, for compound **3**, no temperature independence of the ac susceptibility was observed (χ_M'' maxima moved below 1 Hz at temperatures below 8 K; Figure S4).

The relaxation times of the magnetization (τ) were extracted by fitting Cole–Cole curves (χ'' vs χ') for each temperature with the generalized Debye equation (Figure 5 inset). The relaxation time distribution parameter, α , lies within the range of 0.241–0.438 for all temperatures, which suggests a fairly wide distribution of the relaxation times. The large α parameter and asymmetry of the Cole–Cole curves at some temperatures might suggest the overlap of multiple relaxation processes in **1**. This observation could be due to the two crystallographically unique Dy(III) sites in the solid state structure of **1** having slightly different magnetization dynamics. Additionally, it has

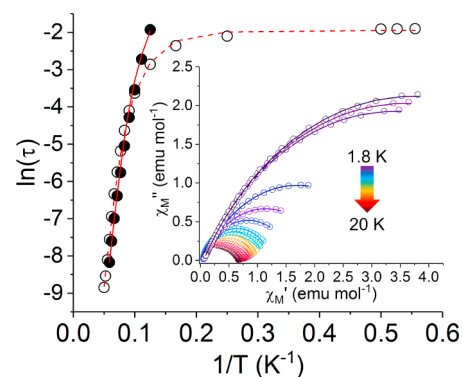


Figure 5. Arrhenius plot of magnetization relaxation time data for **1** (open circles) and **3** (solid circles) in zero dc field. The dashed and solid lines correspond to fits for **1** and **3**, respectively (see text). Inset: Cole–Cole plots for **1** under zero dc field. Solid lines are the best fits to the experimental data, obtained with the generalized Debye model.

recently been emphasized that multiple relaxation events can occur also for single lanthanide sites and can contribute to said asymmetry.¹⁶ The thus extracted relaxation times were used to construct Arrhenius plots ($T = 1.8$ –20 K (for **1**) and 8–17 K (for **3**); Figure 5). The data for **1** was fit (dashed line) including contributions from quantum tunneling, Raman scattering, and Orbach processes according to $\tau^{-1} = \tau_{\text{QTM}}^{-1} + CT^5 + \tau_0^{-1} \exp(-U_{\text{eff}}/k_B T)$. For **3**, no contributions from quantum tunneling were included (solid line). These fit models resulted in a value for the effective barrier to magnetization reversal U_{eff} of 110 cm^{-1} (159 K) for **1** ($\tau_{\text{QTM}} = 0.14 \text{ s}$; $C = 2.9 \times 10^{-4} \text{ s}^{-1} \text{ K}^{-5}$; $\tau_0 = 6.0 \times 10^{-8} \text{ s}$) and 108 cm^{-1} (155 K) for **3** ($C = 2.1 \times 10^{-4} \text{ s}^{-1} \text{ K}^{-5}$; $\tau_0 = 3.3 \times 10^{-8} \text{ s}$).

The observed slow magnetic relaxation for **1** in ac susceptibility measurements would be expected to result in magnetic hysteresis at low temperatures. Magnetization studies of **1** at temperatures between 1.8 and 4.5 K (Figure 6) were

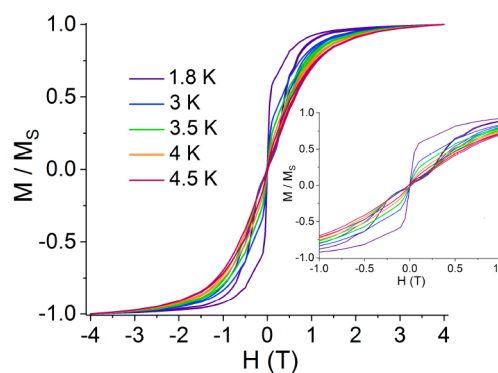


Figure 6. Variable field magnetization data for **1** collected from 1.8 to 4.5 K at a sweep rate of 0.9 mT s^{-1} .

carried out using scan rates of 0.9 mT/s . At 1.8 K, compound **1** displays a waist restricted hysteresis loop, approaching magnetic saturation at 4 T and featuring a step like decrease of the magnetization at zero field. The absence of a coercive field is indicative of QTM processes outpacing the magnetic field sweep rate as has been previously observed.¹⁷ This observation is in good agreement with the temperature independent nature of the χ_M'' between 1.8 and 4 K. The opening in the hysteresis loop steadily decreases upon increasing the temperature and remains only slightly open at 4.5 K.

In conclusion, we introduced the first example of a lanthanide metallocenophane complex. The utilization of this unique ligand for lanthanide binding allows for an approximate trigonal prismatic geometry around the Dy(III) ion in compound **1** as well as short intramolecular distances to Fe(II) ions. Compound **1** displays all characteristics of a soft single-molecule magnet with an effective barrier to magnetization reversal of $\sim 110 \text{ cm}^{-1}$. We are currently investigating potential interactions between the Dy(III) ion and the ferrous sites as well as expanding our studies to other highly anisotropic lanthanide ions. Furthermore, complexes of this new type of heterometallic SMM have the potential to display redox-switchability of their magnetic properties and these investigations will be subject of future studies.

■ ASSOCIATED CONTENT

Supporting Information

The Supporting Information is available free of charge on the ACS Publications website at DOI: 10.1021/jacs.7b01499.

Experimental methods, synthetic details (PDF)

Data for $\text{C}_{38}\text{H}_{40}\text{DyFe}_3\text{Li}_2\text{O}_2$, $\text{C}_{16}\text{H}_{32}\text{LiO}_4$ (CIF)

■ AUTHOR INFORMATION

Corresponding Author

*nippe@chem.tamu.edu

ORCID

Michael Nippe: 0000-0003-1091-4677

Present Address

Department of Chemistry, Texas A&M University, 3255 TAMU, College Station, TX 77843, USA

Notes

The authors declare no competing financial interest.

■ ACKNOWLEDGMENTS

M.N. is grateful to the TAMU Chemistry Department for generous start-up funds and general financial support by the Welch Foundation (A-1880).

■ REFERENCES

- (1) Braunschweig, H.; Kupfer, T. *Acc. Chem. Res.* **2010**, *43*, 455.
- (2) (a) Osborne, A. G.; Whiteley, R. H. *J. Organomet. Chem.* **1975**, *101*, C27. (b) Braunschweig, H.; Dirk, R.; Müller, M.; Nguyen, P.; Resendes, R.; Gates, D. P.; Manners, I. *Angew. Chem., Int. Ed. Engl.* **1997**, *36*, 2338. (c) Pudelski, J. K.; Gates, D. P.; Rulkens, R.; Lough, A. J.; Manners, I. *Angew. Chem.* **1995**, *107*, 1633; *Angew. Chem., Int. Ed. Engl.* **1995**, *34*, 1506. (d) Stoeckli-Evans, H.; Osborne, A. G.; Whiteley, R. H. *J. Organomet. Chem.* **1980**, *194*, 91.
- (3) (a) Braunschweig, H.; Kupfer, T. *Eur. J. Inorg. Chem.* **2012**, *2012*, 1319. (b) Sheridan, J. B.; Lough, A. J.; Manners, I. *Organometallics* **1996**, *15*, 2195. (c) Mizuta, T.; Onishi, M.; Nakazono, T.; Nakazawa, H.; Miyoshi, K. *Organometallics* **2002**, *21*, 717. (d) Braunschweig, H.; Dirk, R.; Englert, U.; Jäkle, F.; Berenbaum, A.; Green, J. C.; Lough, A. J.; Manners, I. *J. Am. Chem. Soc.* **2000**, *122*, 5765. (e) Mizuta, T.; Imamura, Y.; Miyoshi, K. *J. Am. Chem. Soc.* **2003**, *125*, 2068. (f) Herbert, D. E.; Mayer, U. F. J.; Manners, I. *Angew. Chem., Int. Ed.* **2007**, *46*, 5060.
- (4) (a) Bellas, V.; Rehahn, M. *Angew. Chem., Int. Ed.* **2007**, *46*, 5082. (b) Hempenius, M. A.; Cirmi, C.; Lo Savio, F.; Song, J.; Vancso, G. J. *Macromol. Rapid Commun.* **2010**, *31*, 772. (c) Bhattacharjee, H.; Müller, J. *Coord. Chem. Rev.* **2016**, *314*, 114. (d) Hailes, R. L. N.; Oliver, A. M.; Gwyther, J.; Whittell, G. R.; Manners, I. *Chem. Soc. Rev.* **2016**, *45*, 5358.
- (5) Schachner, J. A.; Lund, C. L.; Quail, J. W.; Müller, J. *Organometallics* **2005**, *24*, 785.
- (6) Stoeckli-Evans, H.; Osborne, A. G.; Whiteley, R. H. *Helv. Chim. Acta* **1976**, *59*, 2402.
- (7) Rulkens, R.; Lough, A. J.; Manners, I. *Angew. Chem., Int. Ed. Engl.* **1996**, *35*, 1805.
- (8) Butler, I. R.; Cullen, W. R.; Einstein, F. W. B.; Rettig, S. J.; Willis, A. J. *Organometallics* **1983**, *2*, 128.
- (9) Rulkens, R.; Gates, D. P.; Balaishis, D.; Pudelski, J. K.; McIntosh, D. F.; Lough, A. J.; Manners, I. *J. Am. Chem. Soc.* **1997**, *119*, 10976.
- (10) (a) Broussier, R.; Da Rold, A.; Gautheron, B.; Dromzee, Y.; Jeannin, Y. *Inorg. Chem.* **1990**, *29*, 1817. (b) Whittell, G. R.; Partridge, B. M.; Presly, O. C.; Adams, C. J.; Manners, I. *Angew. Chem., Int. Ed.* **2008**, *47*, 4354. (c) Matas, I.; Whittell, G. R.; Partridge, B. M.; Holland, J. P.; Haddow, M. F.; Green, J. C.; Manners, I. *J. Am. Chem. Soc.* **2010**, *132*, 13279.
- (11) (a) Sängler, I.; Heilmann, J. B.; Bolte, M.; Lerner, H.-W.; Wagner, M. *Chem. Commun.* **2006**, 2027. (b) Garcia-Álvarez, J.; Kennedy, A. R.; Klett, J.; Mulvey, R. E. *Angew. Chem., Int. Ed.* **2007**, *46*, 1105. (c) Blair, V. L.; Carrella, L. M.; Clegg, W.; Klett, J.; Mulvey, R. E.; Rentschler, E.; Russo, L. *Chem. - Eur. J.* **2009**, *15*, 856.
- (12) Bucaille, A.; Le Borgne, T.; Ephritikhine, M.; Daran, J.-C. *Organometallics* **2000**, *19*, 4912.
- (13) (a) Ishikawa, N.; Sugita, M.; Ishikawa, T.; Koshihara, S.; Kaizu, Y. *J. Am. Chem. Soc.* **2003**, *125*, 8694. (b) Jiang, S.-D.; Wang, B.-W.; Sun, H.-L.; Wang, Z.-M.; Gao, S. *J. Am. Chem. Soc.* **2011**, *133*, 4730. (c) Rinehart, J. D.; Fang, M.; Evans, W. J.; Long, J. R. *J. Am. Chem. Soc.* **2011**, *133*, 14236. (d) Meihaus, K. R.; Long, J. R. *J. Am. Chem. Soc.* **2013**, *135*, 17952. (e) Pugh, T.; Chilton, N. F.; Layfield, R. A. *Angew. Chem., Int. Ed.* **2016**, *55*, 11082. (f) Harriman, K. L. M.; Brosmer, J. L.; Ungur, L.; Diaconescu, P. L.; Murugesu, M. *J. Am. Chem. Soc.* **2017**, *139*, 1420. (g) Ding, Y.-S.; Chilton, N. F.; Winpenny, R. E. P.; Zheng, Y.-Z. *Angew. Chem., Int. Ed.* **2016**, *55*, 16071. For recent reviews/perspectives, see: (h) Woodruff, D. N.; Winpenny, R. E. P.; Layfield, R. A. *Chem. Rev.* **2013**, *113*, 5110. (i) Liddle, S. T.; van Slageren, J. *Chem. Soc. Rev.* **2015**, *44*, 6655. (j) Harriman, K. L. M.; Murugesu, M. *Acc. Chem. Res.* **2016**, *49*, 1158.
- (14) Perucha, A. S.; Heilmann-Brohl, J.; Bolte, M.; Lerner, H.-W.; Wagner, M. *Organometallics* **2008**, *27*, 6170.
- (15) Gatteschi, D.; Sessoli, R.; Villain, J. *Molecular Nanomagnets*; Oxford University Press, 2006.
- (16) Ho, L. T. A.; Chibotaru, L. F. *Phys. Rev. B: Condens. Matter Mater. Phys.* **2016**, *94*, 104422.
- (17) Pugh, T.; Chilton, N. F.; Layfield, R. A. *Chem. Sci.* **2017**, *8*, 2073.